Synthetic and Systems Biotechnology 8 (2023) 323–330

Contents lists available at ScienceDirect

Synthetic and Systems Biotechnology

journal homepage: www.keaipublishing.com/en/journals/synthetic-and-systems-biotechnology

Original Research Article

Engineering the thermostability of D-lyxose isomerase from *Caldanaerobius polysaccharolyticus* via multiple computer-aided rational design for efficient synthesis of D-mannose

Hao Wu [a,b], Ming Yi [a], Xiaoyi Wu [a], Yating Ding [a], Minghui Pu [a], Li Wen [a], Yunhui Cheng [a], Wenli Zhang [b,*], Wanmeng Mu [b]

[a] School of Food Science and Bioengineering, Changsha University of Science & Technology, Changsha, 410114, China
[b] State Key Laboratory of Food Science and Technology, Jiangnan University, Wuxi, 214122, China

ARTICLE INFO

Keywords:
D-lyxose isomerase
Thermostability
D-mannose
Molecular modification

ABSTRACT

D-Mannose is an attractive functional sugar that exhibits many physiological benefits on human health. The demand for low-calorie sugars and sweeteners in foods are increasingly available on the market. Some sugar isomerases, such as D-lyxose isomerase (D-LIase), can achieve an isomerization reaction between D-mannose and D-fructose. However, the weak thermostability of D-LIase limits its efficient conversion from D-fructose to D-mannose. Nonetheless, few studies are available that have investigated the molecular modification of D-LIase to improve its thermal stability. In this study, computer-aided tools including FireProt, PROSS, and Consensus Finder were employed to jointly design D-LIase mutants with improved thermostability for the first time. Finally, the obtained five-point mutant M5 (N21G/E78P/V58Y/C119Y/K170P) showed high thermal stability and catalytic activity. The half-life of M5 at 65 °C was 10.22 fold, and the catalytic efficiency towards 600 g/L of D-fructose was 2.6 times to that of the wild type enzyme, respectively. Molecular dynamics simulation and intramolecular forces analysis revealed a thermostability mechanism of highly rigidity conformation, newly formed hydrogen bonds and π-cation interaction between and within protein domains, and redistributed surface electrostatic charges for the mutant M5. This research provided a promising D-LIase mutant for the industrial production of D-mannose from D-fructose.

1. Introduction

Recently, the increasing incidence and prevalence rate of diabetes, obesity, and hypertension have raised widespread concern from the public and society. The occurrence of these chronic diseases is closely related to the intake of high-sugar and fatty food [1]. Consequently, the demand for low-calorie sugars and sweeteners in foods are increasingly available on the market. D-Mannose is an attractive functional sugar that exhibits many physiological benefits, such as inhibiting tumor growth [2], stimulating regulatory T cell differentiation [3], and anti-inflammatory activity [4]. D-Mannose is mainly found in plants in the form of high polymer (mannan) in nature. Therefore, traditionally, extraction of D-mannose from plants was once the main synthetic approach, but this method required the use of strong acids, high temperatures, and high-pressure conditions, resulting in a higher extraction cost [5]. If the chemical strategy is adopted to prepare D-mannose, there are also concerns of high-cost and environmental protection [6]. Thus, enzymatic conversion is favored because of the mild reaction conditions and the production of fewer harmful by-products. Structurally, D-mannose is an aldose isomer of D-fructose. Some sugar isomerases, such as D-lyxose isomerase (D-LIase, EC 5.3.1.15), can achieve an isomerization reaction between D-mannose and D-fructose.

The high thermostability and catalytic efficiency of D-LIase are the most important characteristics, and are prerequisites for the long-term conversion of D-fructose to D-mannose. Additionally, high temperature conditions could accelerate the reaction rate, increase the solubility of the substrate and the product, and reduce the risk of microbial contamination [7]. Therefore, many studies have been devoted to the discovery of novel D-LIases with high thermostability and catalytic efficiency. Until now, many types of D-LIase have been identified and

Peer review under responsibility of KeAi Communications Co., Ltd.
* Corresponding author. State Key Laboratory of Food Science and Technology, Jiangnan University, Wuxi, Jiangsu, 214122, China.
E-mail address: wenlizhang@jiangnan.edu.cn (W. Zhang).

https://doi.org/10.1016/j.synbio.2023.04.003
Received 13 March 2023; Received in revised form 16 April 2023; Accepted 17 April 2023
Available online 21 April 2023
2405-805X/© 2023 The Authors. Publishing services by Elsevier B.V. on behalf of KeAi Communications Co. Ltd. This is an open access article under the CC BY-NC-ND license (http://creativecommons.org/licenses/by-nc-nd/4.0/).

characterized from *Thermofilum* sp. [8], *Thermoprotei archaeon* [9], *Caldanaerobius polysaccharolyticus* [10], *Thermoflavimicrobium dichotomicum* [11], *Bacillus velezensis* [12], *Thermosediminibacter oceani* [13], and so on. Of these, some D-LIases achieve higher catalytic efficiency, such as *C. polysaccharolyticus* (conversion rate 25.6% with 45% enzyme activity retained at 65 °C after incubation for 3 h) [10], *T. dichotomicum* (conversion rate 24.2% and half-life 1.45 h at 65 °C) [11], and *S. proteamaculans* (conversion rate 20% and half-life 0.09 h at 50 °C) [14]. However, the thermal stability of these enzymes was weak and could not achieve a long-term conversion to produce D-mannose from D-fructose. Although high thermostable D-LIase (EC 5.3.1.15) was identified from the hyperthermophilic archaeon *Thermofilum* sp. that could retain 60% of its original activity after 60 min of incubation at 80 °C, but this enzyme achieved less than 2% activity towards D-mannose [8]. As a result, it remains a challenge for obtaining D-LIases with high thermostability and catalytic efficiency. By comparison with gene mining, molecular modification of the D-LIase via protein engineering may represent an alternative method to improve its thermostability accompanying with high catalytic efficiency. *C. polysaccharolyticus* D-LIase (Capo-D-LIase) may act as a biocatalyst with high catalytic efficiency; however, the thermal stability of the enzyme is slightly weak [10]. Nonetheless, few studies are available that have investigated the molecular modification of D-LIase to improve its thermal stability. Thus, the molecular modification of D-LIase by a protein engineering technique to improve its thermal stability is of great significance for efficient production of D-mannose.

In this study, computer-aided rational design tools were employed to improve the thermostability of Capo-D-LIase on the basis of its sequence and structural properties. The FireProt, PROSS, and Consensus Finder server was used for the first time to jointly design D-LIase mutants. Finally, compared to wild type Capo-D-LIase, a mutant M5 containing five altered residues (N21G/E78P/V58Y/C119Y/K170P) showed a remarkable improvement in thermostability and enhancement in catalytic activity. The thermostability mechanism was also revealed by amino acid analysis and molecular dynamics simulations.

2. Material and methods

2.1. Strains, plasmids, and reagents

The *E. coli* strain BL21 (DE3) and pET-22b(+) were obtained from our laboratory, which was bought from Sangon Biotech Co., Ltd. (Shanghai, China). *E. coli* DH5α was used as the host for gene cloning. Ampicillin and isopropyl-*β*-D-thiogalactoside (IPTG) were purchased from Sangon Biotech Co., Ltd. (Shanghai, China). Standard samples of D-fructose and D-mannose were purchased from Sigma (St. Louis, MO, USA). Other reagents, including yeast extract, peptone, and sodium chloride were of analytical grade. Ni^{2+} affinity Sepharose (Fast Flow) column was purchased from GE Healthcare, Co., Ltd. (Uppsala, Sweden). Protein gel electrophoresis kit and standard protein marker were purchased from Shanghai Yase Biotechnology Co., Ltd.

2.2. Homology modeling of Capo-D-LIase and the M5 mutant

The AlphaFold program was used to construct the Capo-D-LIase and M5 mutant models based on their amino acid sequences, to obtain three-dimensional structure models that could be used for the subsequent design of mutants and molecular dynamics simulations [15]. Next, the quality of the protein model was evaluated using the PROCHECK program [16].

2.3. Computer-aided rational design for generation of Capo-D-LIase mutants

To improve the thermostability of Capo-D-LIase, we used three online web server tools to design the mutant, respectively, based on its protein sequence or three-dimensional structure. The Consensus Finder (http://kazlab.umn.edu/) is a free web tool that can be used to predict potentially stabilizing mutations by mutating a protein to mimic the consensus sequence of homologs [17]. PROSS (https://pross.weizmann.ac. il/step/pross-terms/) is an automatic algorithm used to evaluate protein stability [18]. FireProt (https://loschmidt.chemi.muni.cz/fireprotweb/) is another web server used for the automatic design of multi-point mutant proteins with high thermostability based on structural and evolutionary information [19]. Amino acid sequences of Capo-D-LIase (GenBank: WP_026486773.1, EC 5.3.1.15) were obtained from the NCBI database. Next, amino acid sequences encoding the three-dimensional structure of Capo-D-LIase were uploaded to the aforementioned web-server to design potential mutants with higher thermostability. Finally, the mutation sites obtained from the three websites were compared and analyzed, and an intersection strategy was adopted to obtain the final mutation sites.

2.4. Construction, expression, and purification of Capo-D-LIase mutants

The primers used for the construction of Capo-D-LIase mutants were designed by SnapGene software and were listed in Table S1. The pET-22b(+) plasmid that harbored the Capo-D-LIase gene was constructed in our laboratory and was used as a template to prepare the mutant plasmid. The PCR products were digested by the DpnI restriction nuclease and transformed into *E. coli* DH5α competent cells by heat shock at 42 °C. The confirmation of all coding mutations was determined by DNA sequencing. Next, the successfully mutant gene harbored in the pET-22b(+) plasmid was transformed into *E. coli* BL21(DE3) to produce the Capo-D-LIase mutant vector. A positive colony exhibiting ampicillin resistance was selected after streaking on a Luria-Bertani agar plate, which was then isolated and inoculated into another 4 mL of Luria-Bertani medium containing 100 μg/mL of ampicillin for pre-incubation at 37 °C under shaking (200 rpm). After an initial growth culture of 12–14 h, the 4 mL seed culture was transferred to fresh 200 mL of Luria-Bertani medium containing 100 μg/mL of ampicillin for incubation at 37 °C under shaking (200 rpm) until the optimal density at 600 nm of 0.6–0.8 was reached. Subsequently, a final concentration of 1 mM IPTG was added to the medium to induce the overexpression of Capo-D-LIase mutant at 28 °C under shaking (200 rpm) for 6–8 h.

The purification steps of Capo-D-LIase mutants were as follows. Unless otherwise stated, all operating conditions were performed under controlled conditions at 4 °C. First, *E. coli* BL21(DE3) cells containing recombinant pET-22b(+)-Capo-D-LIase plasmid were harvested from culture medium by centrifugation at 10,000×*g* for 15 min. Next, the harvested cells were resuspended in a 20 mL potassium phosphate buffer (PBS–K, 50 mM, pH 7.0) containing 100 mM NaCl, and sonicated for 15 min in 1 s work mode and 2 s pause mode to lyse cells. Subsequently, the ultrasound treated solution was centrifuged at 10,000×*g* for 15 min to remove the cell debris and the obtained supernatant was filtered through a 0.22-μm membrane (Millipore, Shanghai, China). The supernatant was then loaded onto a Ni^{2+} affinity Sepharose (Fast Flow) column that had been equilibrated with PBS-K (50 mM, pH 7.0) containing 500 mM NaCl. Subsequently, washing buffer containing 500 mM NaCl and 90 mM imidazole dissolved in PBS-K (50 mM, pH 7.0) was applied to the column, to remove weakly bound proteins. The target Capo-D-LIase and its mutants harboring the 6 × histidine tags were eluted by the PBS-K solution (50 mM, pH 7.0) containing 500 mM of NaCl and 500 mM of imidazole. Finally, the collected solution was dialyzed twice in the PBS-K solution (50 mM, pH 7.0) to remove excess imidazole.

2.5. Activity assay of the Capo-D-LIase mutants

Mutant enzyme activity was measured in the 0.5 mL solution of PBS-K (50 mM, pH 6.5) solution containing 100 mM of D-fructose, 100 μg/mL of Capo-D-LIase, and 1 mM of Mn^{2+}. The reaction was initiated in the

above system at 65 °C for 15 min, and then terminated by boiling for 15 min. Subsequently, the solution was centrifuged at 8,000×*g* for 15 min and the supernatant was filtered through a 0.22-μm membrane (Millipore, Shanghai, China). The amount of D-fructose and D-mannose was measured at 85 °C by an HPLC system (Waters e2695, Milford, MA, USA) consisting of a refractive index detector and a Carbomix Ca-NP10 column (10 μm, 7.8 mm × 300 mm, Sepax Technologies, Inc., Newark, DE, USA) with a flow rate of 0.6 mL/min and a mobile phase of ultrapure water. One unit (U) of D-LIase was defined as the production of 1 μM of D-mannose from D-fructose per minute under the reaction conditions. The D-LIase mutants with higher enzyme activity and/or thermostability than that of the wild type enzyme were selected as the research target.

2.6. Thermostability and kinetic stability determination of the D-LIase mutants

To determine whether the thermo- and structural stability of the D-LIase mutants were better than that of the wild type enzyme, the melting point temperature (T_m), half-life ($t_{1/2}$), and optimal temperature (T_{opt}) were measured and compared. The T_m values of the D-LIase single point mutant (N21G, V58Y, E78P, R108P, H114E, C119Y, K170P), multi-point mutant M2 (V58Y/E78P), M3 (M2/C119Y), M4 (M3/N21G), M5 (M4/K170P) and wild type Capo-D-LIase were measured using a differential scanning calorimetry instrument (Nano DSC III, New Castle, DE). Operating parameters were set as follows: scan temperature range of 30–110 °C, heating rate of 1 °C/min, pressure of 3 atm. Before loading the enzyme sample, a dialysis buffer was used to correct the baseline line five times. The results of T_m operations were fit and processed using the Nano-Analyze software.

Table 1
The mutation results of thermal stability of D-LIase from *C. polysaccharolyticus* using different algorithms server.

Amino acids		PROSS	Consensus Finder	Fireprot	Selected mutants
Site	Wild Type	Designed Mutant			
3	F	×	R	×	☒
9	L	×	A	×	☒
14	Y	A	L	×	☒
21	N	G	×	G	N21G
24	I	×	×	L	☒
35	A	×	×	F	☒
42	I	L	×	×	☒
45	T	V	×	×	☒
48	Q	×	×	M	☒
50	V	L	×	×	☒
53	V	×	×	L	☒
56	E	×	×	D	☒
58	V	Y	×	Y	V58Y
75	K	R	×	×	☒
78	E	P	P	P	E78P
82	K	E	×	×	☒
106	Q	E	P	×	☒
108	R	P	×	P	R108P
111	N	H	×	×	☒
114	H	E	E	×	H114E
119	C	Y	×	Y	C119Y
123	F	×	×	W	☒
126	V	×	×	I	☒
129	N	K	×	×	☒
137	M	P	×	×	☒
141	L	W	×	×	☒
148	E	P	×	×	☒
158	T	×	×	S	☒
161	M	×	R	×	☒
166	V	×	×	I	☒
170	K	×	P	P	K170P
Selection probability		6/18	3/8	6/15	7

To determine the $t_{1/2}$ value, the D-LIase mutants (M2, M3, M4, M5) and wild type Capo-D-LIase were incubated at 65 °C (T_{opt} of wild type Capo-D-LIase) in the PBS-K system (50 mM, pH 6.5) containing 100 mM of D-fructose, 100 μg/mL of enzyme and 1 mM of Mn^{2+} in advance, and sampled at different incubation time to investigate its residual activity. The initial activity of wild type Capo-D-LIase (unincubated) was defined as 100% and the activities of the D-LIase mutants were calculated as relative activity (%) to the initial activity of Capo-D-LIase. The $t_{1/2}$ value was calculated according to the formula ($t_{1/2} = \ln 2/kd$), in which the decay constant (kd) was determined by the first-order linear regression with the equation: $\ln A = -kd \times t$ (A: residual activity; t: incubation time) [20].

To evaluate changes in the T_{opt} of mutants M4 and M5 (with improved thermostability), both mutants together with wild type Capo-D-LIase were exposed to different temperatures (55–75 °C) for the activity assay. The T_{opt} was determined from the group that exhibited the highest activity. The Capo-D-LIase activity at 65 °C was defined as 100% and M4 and M5 activities were calculated as relative activity (%) to that of Capo-D-LIase activity at 65 °C.

2.7. Molecular dynamics simulation of Capo-D-LIase and M5 mutant

Molecular dynamics (MD) simulation was performed using the Gromacs 2018.4 program under constant temperature, constant pressure, and periodic boundary conditions. The Amber14SB all-atomic force field and TIP3P water model were applied [21]. During the MD simulation process, all bonds involving hydrogen atoms were constrained by the LINCS algorithm, and the integral step was 2 fs. The electrostatic interaction was calculated using the particle mesh Ewald PME method [22]. The cutoff value for the non-bond interaction was set to 10 Å and updated every 10 steps. The V-rescale temperature coupling method was used to control the simulated temperature of 338.15K, and the Parrinello-Rahman method was used to control the pressure of 1 bar [23]. First, the steepest descent method was used to minimize the energy of the two systems to eliminate the close contact between atoms. Then, NVT and NPT equilibria of 1 ns were simulated at 338.15 K. Finally, the MD simulation of 50 ns was performed on the system, and conformation was saved every 10 ps. The visualization of the simulation results was completed using a Gromacs embedded program and VMD software.

2.8. Enzymatic synthesis of D-mannose from D-fructose

D-Mannose synthesis was carried out at 65 °C for 24 h in the 500 mL PBS-K system (50 mM, pH 6.5) containing 600 g/L of D-fructose, 100 μg/mL of enzyme and 1 mM of Mn^{2+}. The mutant M5 with the highest thermostability was used to compare the production efficiency with Capo-D-LIase. The reaction was sampled at various intervals to determine the D-mannose yield by HPLC as stated above.

3. Results and discussion

3.1. Why choose computer-aided tools to improve thermal stability of proteins

With the advancement of in-depth understanding of protein structure function and catalytic mechanism, a variety of computational design methods have been used to improve the thermal stability of enzymes, including homologous sequence alignment, protein conformational free energy calculation [24], disulfide bond design [25], proline effect [26], temperature factor design [27], and hydrophobic cavity packaging [28]. However, it is often difficult for researchers to select which strategy to apply to improve the thermal stability of enzymes. The accuracy of protein stability predictions can often be performed using websites that integrate many design tools and protein engineering strategies, such as the Consensus Finder [17], PROSS [18] and FireProt server [19]. For example, the thermostability and catalytic activity of the

glycosyltransferase mutant Mut8 was improved after using the FireProt server for calculations, which integrated FoldX and Rosetta tools [29]. Furthermore, the design of the PROSS algorithm also successfully increased the activity and stability of the ^{S136E}PETase variant based on its sequence and structure information [30]. However, these algorithms have maintained a certain degree of independence and have not been combined to improve the overall thermal stability of proteins.

3.2. Homology modeling structure analysis

Ramachandran plot is used to describe the degree of rotation of the bond between alpha carbon atoms and carbonyl carbon atoms in peptide bonds in the three-dimensional structure of proteins or peptides, and mainly indicates the allowed and disallowed conformations of amino acid residues in proteins or peptides. The Ramachandran plot is divided into three areas: full permit zone (red zone), permit zone (yellow zone), and disallow zone (blank zone). The results of the Ramachandran plot analyses of Capo-D-LIase are shown in the Supplementary Materials Fig. S1. The amino acids in the fully permitted zone accounted for 91.1%, and the amino acids in the permitted zone accounted for 8.9%, and the summed amino acids exceeded 95%. No amino acid residues were located in the torsion forbidden zone. These results suggested that the dihedral angles of all amino acid residues of Capo-D-LIase were within a reasonable range, which was consistent with the stereochemical energy rule. The three-dimensional structure was also used for the subsequent study.

3.3. Rational design of the Capo-D-LIase mutants aided by computer-aided tools

Consensus Finder is a web server that mainly performs multiple sequence alignment to predict stabilizing substitutions in proteins by replacing a rarely occurring amino acid with a frequently occurring amino acid [17]. After inputting the FASTA file of the wild type Capo-D-LIase, the web server generated eight potential mutants including F3R, L9A, Y14L, E78P, Q106P, H114E, M161R, K170P (Table 1). Based on the uploaded three-dimensional structure and amino acid sequence in the PROSS server, 18 potential mutants including Y14A, N21G, I42L, T45V, V50L, V58Y, K75R, E78P, K82E, Q106E, R108P, N111H, H114E, C119Y, N129K, M137P, L141W, E148P (Table 1) were generated. The Fireprot server supported uploading protein structure or amino acid sequence on the web and determined mutations outside of the active amino acid site. Therefore, 15 potential mutants including N21G, I24L, A35F, Q48 M, V53L, E56D, V58Y, E78P, R108P, C119Y, F123W, V126I, T158S, V166I, and K170P (Table 1) were designed. Thus, different computational servers defined different mutant designs for the same enzyme. In this study, to improve the accuracy of selection of potential mutation sites, we adopted the intersection strategy, that is, we selected the same mutation predicted by at least two servers as potential candidate mutants among all the mutants defined by the three servers. Therefore, seven mutants, such as N21G, V58Y, E78P, R108P, H114E, C119Y, and K170P (Table 1) were selected from all 41 mutants as follow-up experiments. The intersection strategy can effectively avoid the accuracy deficits of using a single-server design, thus greatly increasing the accuracy of mutations and avoiding excessive experiments.

3.4. Thermostability analysis of Capo-D-LIase mutants

Thermodynamic stability is a property generally used to characterize the tendency for protein unfolding. The protein structure is in a relatively stable energy state determined by entropy and enthalpy, and the tendency to unfold is not a spontaneous process. Natural enzymes usually evolve into a thermodynamically stable state to adapt to ambient temperatures [31]. The structural stability of the Capo-D-LIase and its mutants, including N21G, V58Y, E78P, R108P, H114E, C119Y, and K170P, were assessed by the T_m values measured using the Nano DSC instrument. As shown in Fig. 1, compared to wild type Capo-D-LIase, the T_m values of the N21G, C119Y, and K170P mutants increased by more than 0.5 °C, while the T_m values of the V58Y, E78P and R108P mutants decreased by more than 0.5 °C. Interestingly, the T_m value of the H114E mutant was changed by less than 0.5 °C. These results indicated that the structural stability of the N21G, C119Y, and K170P mutants was enhanced, whereas that of the V58Y, E78P, and R108P mutants was reduced. Furthermore, by comparison with Capo-D-LIase, the relative activity of the N21G, V58Y, E78P, C119Y, and K170P mutants was increased by 0.23-, 1.4-, 1.04-, 1.17-, 0.90-fold, respectively, whereas the relative activity of the R108P and H114E mutants was 107.12% and 93.11% that of Capo-D-LIase (Table 2). Combining the results of structural stability and relative enzyme activity, the mutants R108P and H114E were not suitable for the next round of mutations. The single-point mutants N21G, V58Y, E78P, C119Y, and K170P with higher enzyme activity and/or thermostability were selected and combined for multi-point mutant preparation.

Firstly, the single-point mutants V58Y and E78P, having a lower T_m value and higher enzyme activity compared to wild type Capo-D-LIase, were combined to prepare the double-point mutant M2 (V58Y/E78P).

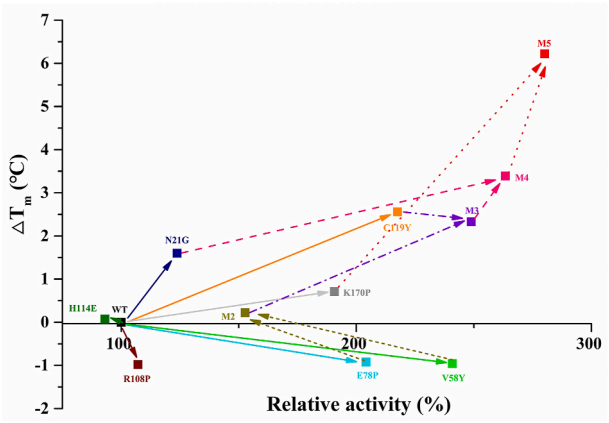

Fig. 1. Changes in T_m values and relative enzyme activity in single- and multi-point mutants.

Table 2
The T_m value and relative activity of wild type enzymes and different mutants.

Enzymes	T_m values (°C)	Relative activity (%)
WT	76.23	100.0 ± 3.46
N21G	77.83 ↑	123.77 ± 3.11 ⇈
V58Y	75.27 ↓	240.87 ± 9.48 ⇈
E78P	75.31 ↓	204.13 ± 15.86 ⇈
R108P	75.25 ↓	107.12 ± 0.34 ⇉
H114E	76.30 →	93.11 ± 12.13 ⇉
C119Y	78.79 ↑	217.57 ± 19.32 ⇈
K170P	76.94 ↑	190.70 ± 15.20 ⇈
M2	76.45 →	153.78 ± 3.70 ⇈
M3	78.56 ↑	251.74 ± 6.58 ⇈
M4	79.62 ↑	266.57 ± 5.34 ⇈
M5	82.45 ↑	283.72 ± 0.82 ⇈

"↑" indicates the T_m value is 0.5 °C higher than that of wild type enzyme.
"↓" indicates the T_m value is 0.5 °C lower than that of wild type enzyme.
"→" indicates the T_m value does not change over 0.5 °C when compared with wild type enzyme.
"⇈" indicates the enzyme activity is more than 20% higher than wild type enzyme.
"⇉" indicates the enzyme activity changes less than 20% when compared with wild type enzyme.
WT: wild type enzyme D-LIase from *C. polysaccharolyticus*; M2: E78P/V58Y; M3: E78P/V58Y/C119Y; M4:N21G/E78P/V58Y/C119Y; M5: N21G/E78P/V58Y/C119Y/K170P.

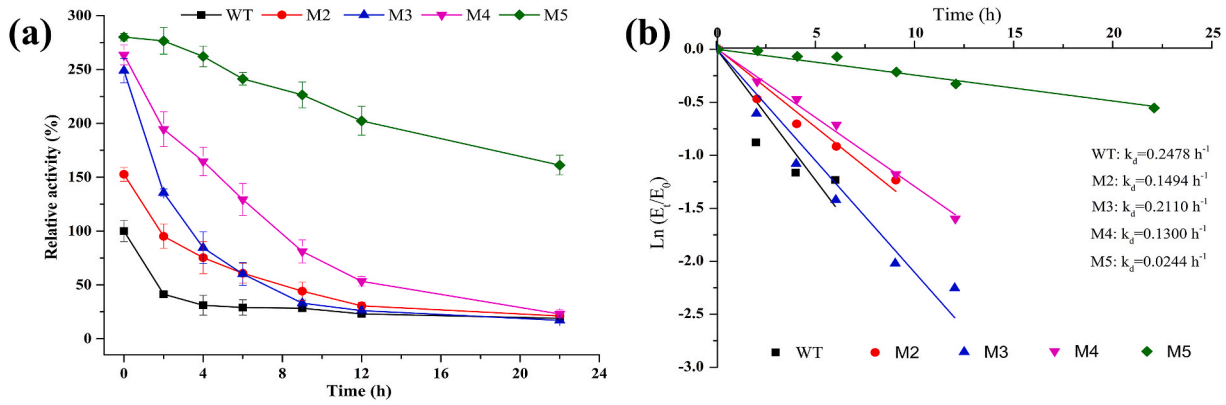

Fig. 2. Thermostability and kinetic stability of Capo-D-LIase and its mutants. **(a)** Thermostability of Capo-D-LIase and its mutants at 65 °C for different time. **(b)** Kinetic stability of Capo-D-LIase and its mutants. WT: *Caldanaerobius polysaccharolyticus* D-LIase; M2: two-point mutant of D-LIase (E78P/V58Y); M3: three-point mutant of D-LIase (E78P/V58Y/C119Y); M4: four-point mutant of D-LIase (N21G/E78P/V58Y/C119Y); M5: five-point mutant of D-LIase (N21G/E78P/V58Y/C119Y/K170P).

Subsequently, the progressive accumulation of mutations was successively constructed using the single-point mutants C119Y, N21G, and K170P, generating mutants M3 (M2/C119Y), M4 (M3/N21G), and M5 (M4/K170P), respectively. As shown in Fig. 1 and Table 2, the structural stability of the multi-point mutants M2, M3, M4, and M5 was strengthened, with 0.22 °C, 2.33 °C, 3.39 °C, and 6.22 °C higher T_m values, respectively, than that of Capo-D-LIase. Correspondingly, the relative activity was increased by 0.54-, 1.52-, 1.67-, and 1.84-fold to that of Capo-D-LIase activity, respectively.

3.5. Kinetic stability analysis of the D-LIase mutants

Kinetic stability refers to the time or temperature required for a protein to retain half its activity when it is in an irreversible state [32]. The kinetic stability of the enzyme can be evaluated by the $t_{1/2}$ value (the time when the enzyme loses half its activity) and kd value (decay constant) that are calculated from the residual activity after incubation at specific temperature for different time. To investigate the kinetic stability of Capo-D-LIase and its mutants M2, M3, M4, and M5, these enzymes were incubated at 65 °C for different time periods and enzyme activity was sampled at fixed time to measure residue activity. As shown in Fig. 2a, the residual activity of Capo-D-LIase had decreased to approximately 30% of the original enzyme activity after incubation at 65 °C after 4 h, while the M2 and M3 mutants achieved 8 h longer activity than Capo-D-LIase. Furthermore, the relative enzyme activity of the M5 mutant remained 1.5 times that of Capo-D-LIase and still remained approximately 53% of its original enzyme activity after incubation for 22 h. These results suggested that the kinetic stability of the M2, M3, M4, and M5 mutants was significantly improved, especially that of the M5 mutant.

In addition, the kd values of Capo-D-LIase, and those of M2, M3, M4, and M5 mutants, were acquired by fitting the residual activity data at various incubation time according to the formula ln A = - kd × t (A: residual activity; t: incubation time). The kd values obtained are shown in Fig. 2b. The value of $t_{1/2}$ at 65 °C was calculated according to the formula ($t_{1/2}$ = ln2/kd), with 2.78, 4.64, 3.26, 5.53, and 28.41 h for Capo-D-LIase, M2, M3, M4, and M5, respectively. The half-lives of the $t_{1/2}$ of mutants M2, M3, M4, and M5 were 1.67, 1.17, 1.99, and 10.22 times longer than those of Capo-D-LIase. These results demonstrated that the thermostability of M4 and M5 mutants was greatly improved. Furthermore, the T_{opt} values for M4 and M5 mutants were also determined at temperatures ranging from 55 °C to 75 °C in the PBS-K (50 mM, pH 6.5) system containing 100 mM of D-fructose, 100 μg/mL of enzyme, and 1 mM of Mn^{2+}. The T_{opt} of M4 and M5 did not change under these conditions, and were consistent with the T_{opt} (65 °C) of Capo-D-LIase (shown in the Supplementary Materials Fig. S2).

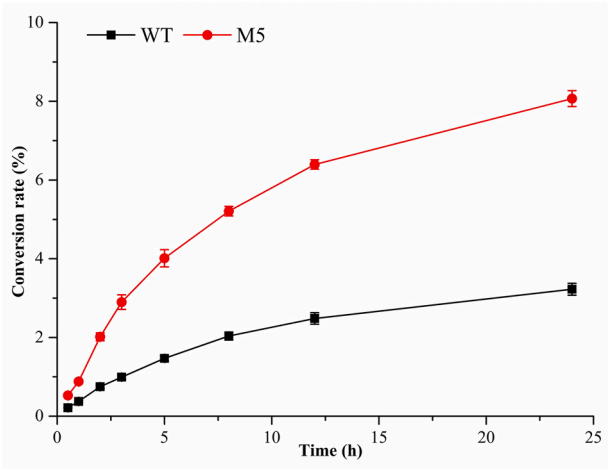

Fig. 3. Time courses of D-mannose production from D-fructose by wild-type enzyme and the M5 mutant. The reaction was performed at 65 °C in the 0.5 L PBS-K (50 mM, pH 6.5) systems that were composed of 600 g/L of D-fructose, 100 μg/mL of enzyme, and 1 mM of Mn^{2+}.

3.6. D-Mannose production by Capo-D-LIase and the M5 mutant enzyme

D-Mannose production from its substrate D-fructose was performed at 65 °C in the 0.5 L PBS-K (50 mM, pH 6.5) system that was composed of 600 g/L of D-fructose, 100 μg/mL of enzyme, and 1 mM of Mn^{2+}. As shown in Fig. 3, the conversion rate of D-mannose from D-fructose catalyzed by M5 mutant was significantly higher than that of the Capo-D-LIase with a prolonged reaction time. After continuous monitoring for 24 h, it was found that the D-mannose content in the M5 system was approximately 2.6 times higher than that of the Capo-D-LIase system. This improvement could be attributed to the high thermal stability of the M5 mutant, which allowed the M5 mutant to maintain high activity to catalyze D-fructose to D-mannose for a prolonged period.

3.7. Molecular mechanism analysis of thermal stability enhancement for the M5 mutant

To further reveal the molecular mechanism underlying the improvement in thermostability of the M5 mutant, MD was used to analyze the root mean square deviation (RMSD) and the root mean square fluctuation (RMSF) of M5 and Capo-D-LIase at 338.15 K for 50 ns. The structure of the M5 mutant was constructed using the AlphaFold

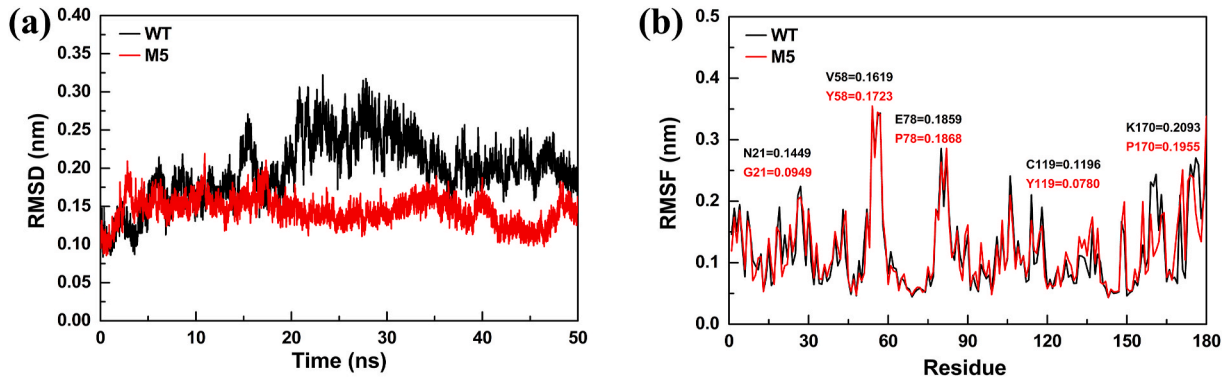

Fig. 4. MD simulations of the wild-type enzyme and its mutant M5. **(a)** RMSD; **(b)** RMSF.

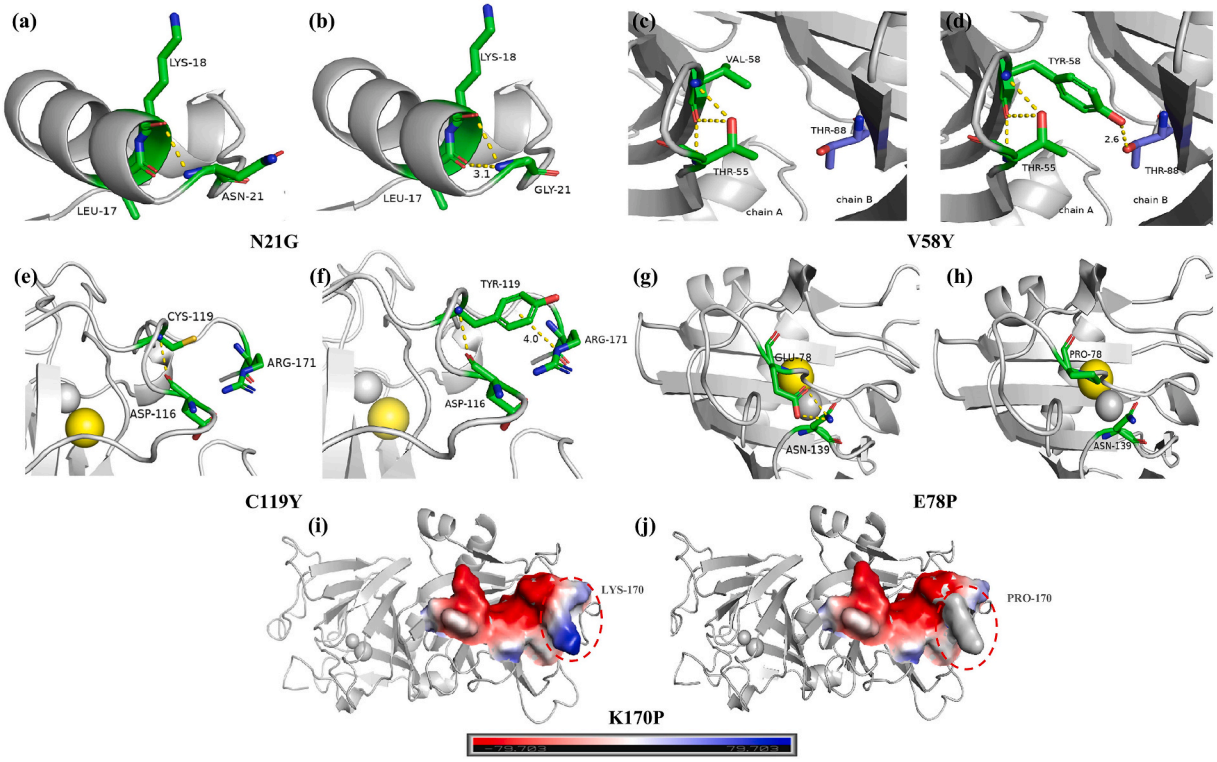

Fig. 5. Structural analysis for the mutation effects on the thermostability of mutant M5. **(a)** Detailed view of the ASN-21 residue in wild-type enzyme. **(b)** Detailed view of the GLY-21 residue in M5. A new hydrogen bond was formed between the G21 and L17 residues. **(c)** Detailed view of the VAL-58 residue in the wild-type enzyme. **(d)** Detailed view of the TRY-58 residue in wild-type enzyme. TYR-58 belonging to A chain and THR-88 belonging to B chain also formed a new hydrogen bond at the submit interface. **(e)** Detailed view of the CYS-119 residue in the wild-type enzyme. **(f)** Detailed view of the residue TYR-119 in M5. The residues TRY-119 and ARG-171 could form π-cation interaction. **(g)** Detailed view of the GLU-78 residue in the wild-type enzyme. The residues GLU-78 and ASN-139 could form hydrogen bond interaction. **(h)** Detailed view of the PRO-78 residue in M5. **(i)** Detailed view of the LYS-170 residue in wild-type enzyme. **(j)** Detailed view of the PRO-170 residue in M5. The surface electrostatic charge distribution was changed after the replacement of positive charged LYS-170 with uncharged PRO-170.

program and its quality was verified using the Ramachandran plot (Fig. S1). As shown in Fig. 4a, the RMSD of the M5 and Capo-D-LIase increased slightly at the beginning of the entire simulation and then stabilized for a short period of time. After 15 ns, the changes in RMSD of the two systems showed significant differences, and the RMSD of the Capo-D-LIase system increased again and fluctuated greatly, while the RMSD of the M5 system remained stable and only fluctuated slightly. The mean RMSDs of Capo-D-LIase and M5 systems were 0.198 ± 0.042 nm and 0.144 ± 0.018 nm, respectively, suggesting that the structure of the M5 mutant was more stable than that of Capo-D-LIase. The RMSF values of all amino acids in the Capo-D-LIase and M5 mutant systems are shown in Fig. 4b. According to the overall trend of change in RMSF, the M5 system had slightly lower RMSF values than that of Capo-D-LIase. Subsequently, the flexibility at the mutation site was analyzed. It was found that the flexibility of mutation sites N21G, C119Y, and K170P decreased, whereas the flexibility of V58Y increased and E78P remained almost unchanged. These results suggested that the thermostability of M5 was greatly enhanced, which was consistent with the aforementioned thermostability data.

The thermal stability of enzymes has been reported to be related to the rigidity and flexibility of the amino acid residues comprising its structure, as well as the complex interaction forces formed between amino acid residues, such as the hydrogen bonds, salt bridges, hydrophobic interactions, and disulfide bonds [32]. To fully understand the thermostability mechanism of the M5 mutant, the intramolecular forces of the amino acids were analyzed and compared for M5 and

Capo-D-LIase. As shown in Fig. 5a and **b**, a new hydrogen bond was formed between the G21 and L17 residue when N21 was replaced by G21. For the V58Y mutation, the Tyr-58 belonging to the A chain and Thr-88 belonging to the B chain also formed a new hydrogen bond at submit interface (Fig. 5d). Compared with Val-58 residue (Fig. 5c), Tyr-58 resulted in a larger steric hindrance space, which made it possible to interact with Thr-88 in the B chain. Furthermore, the residues of C119 and R171 were located in the loop region of the Capo-D-LIase (Fig. 5e), and the mutated Y119 residue generated a π-cation interaction with R171 (Fig. 5f), thus reducing the flexibility of the two loop regions. These newly formed interaction forces between amino acids may be the reason for the enhanced thermal stability. Although the T_m value of the single-point mutant V58Y was slightly lower than that of the wild-type enzyme; the cumulative mutation with other amino acids was indeed beneficial to enhance the structural stability of Capo-D-LIase. Furthermore, after E78 was replaced by P78, the hydrogen bond originally formed with N139 disappeared in mutant E78P (Fig. 5g and h), which was consistent with the results of the structural thermal stability test of the single-point mutant E78P, but this mutation improved catalytic activity. Since the E82 residues constituted the metal ion binding center of the wild enzyme, we speculated that the existing E78 would interfere with the binding between the substrate and metal ions, thus affecting the activity, and the glutamate mutation would be conducive to improvement of activity. Similar studies have found that amino acid residues surrounding the active center can affect its entry by forming hydrogen bonds with the substrate [33]. When analyzing the K170P mutant, it was found that the residue of K170 was located at the end of C-terminal loop region, and no new interaction force was formed between K170 and its surrounding amino acids after it was mutated into proline (Fig. 5i and j). However, the distribution of charge on the surface of M5 and Capo-D--LIase changed markedly. Optimizing the interaction between protein surface charges and eliminating electrostatic repulsion has been reported to improve the thermal stability of enzymes [34]. The K170 residue was located at the C-terminal with a positive charge, which may lead to positive charge repulsion, thus resulting in enzyme instability. When the positively charged residue lysine is mutated to neutral residue proline, it may help reduce the positive charge in this region, thus improving the thermal stability of the enzyme.

4. Conclusion

In this study, computer-aided tools including FireProt, PROSS, and Consensus Finder servers were first used to jointly design D-LIase mutants to improve its thermostability based on amino acid sequence and structure property. This strategy was proven to be a very efficient and effective method. From the seven designed single-point mutants, five mutation sites with significant improvement in thermal stability and/or catalytic activity were selected for cumulative mutation. Finally, the obtained five-point mutant M5 (N21G/E78P/V58Y/C119Y/K170P) had high thermal stability and catalytic activity. The half-life of M5 at 65 °C was 10.22 fold, and the catalytic efficiency towards 600 g/L of D-fructose was 2.6 times to that of the wild type Capo-D-LIase, respectively. This research provided a new strategy for molecular modification of the thermal stability of D-LIase and presented a promising D-LIase mutant for the industrial production of D-mannose from D-fructose.

CRediT authorship contribution statement

Hao Wu: Conceptualization, Investigation, Methodology and wrote original manuscript. Ming Yi and Xiaoyi Wu: Methodology, investigation and formal analysis, corrected the original manuscript and data processing and data curation. Yating Ding and Minghui Pu: reviewed and edited the draft. Li Wen and Yunhui Cheng: gave major comments and reviewed the manuscript. Wenli Zhang and Wanmeng Mu: project administration.

Declaration of competing interest

The authors declare that they have no known competing financial interests or personal relationships that could have appeared to influence the work reported in this paper.

Acknowledgements

This work was supported by the National Natural Science Foundation of China (32201963), and Scientific Research Foundation of Hunan Provincial Education Department (22C0137). We appreciate Phadcalc (https://www.phadcalc.com/) for the molecular docking simulation.

Appendix A. Supplementary data

Supplementary data to this article can be found online at https://doi.org/10.1016/j.synbio.2023.04.003.

References

[1] Zhang W, Zhang T, Jiang B, Mu W. Enzymatic approaches to rare sugar production. Biotechnol Adv 2017;35(2):267–74.
[2] Gonzalez PS, O'Prey J, Cardaci S, Barthet VJA, Sakamaki J-i, Beaumatin F, Roseweir A, Gay DM, Mackay G, Malviya G, Kania E, Ritchie S, Baudot AD, Zunino B, Mrowinska A, Nixon C, Ennis D, Hoyle A, Millan D, McNeish IA, Sansom OJ, Edwards J, Ryan KM. Mannose impairs tumour growth and enhances chemotherapy. Nature 2018;563(7733):719–23.
[3] Zhang D, Chia C, Jiao X, Jin W, Kasagi S, Wu R, Konkel JE, Nakatsukasa H, Zanvit P, Goldberg N, Chen Q, Sun L, Chen Z-J, Chen W. D-mannose induces regulatory T cells and suppresses immunopathology. Nat Med 2017;23(9):1036–45.
[4] Torretta S, Scagliola A, Ricci L, Mainini F, Di Marco S, Cuccovillo I, Kajaste-Rudnitski A, Sumpton D, Ryan KM, Cardaci S. D-mannose suppresses macrophage IL-1β production. Nat Commun 2020;11(1):6343.
[5] Fan S-P, Jiang L-Q, Chia C-H, Fang Z, Zakaria S, Chee K-L. High yield production of sugars from deproteinated palm kernel cake under microwave irradiation via dilute sulfuric acid hydrolysis. Bioresour Technol 2014;153:69–78.
[6] Zhang W, Zhang C, Liang G. Study on increasing yield of D-mannose from D-glucose by epimerization conversion (In Chinese), Technol. Dev. Chem. Ind. 2017;46(3):18–21.
[7] Wu H, Zhang W, Mu W. Recent studies on the biological production of D-mannose. Appl Microbiol Biotechnol 2019;103(21):8753–61.
[8] De Rose SA, Kuprat T, Isupov MN, Reinhardt A, Schönheit P, Littlechild JA. Biochemical and structural characterisation of a novel D-lyxose isomerase from the hyperthermophilic archaeon *Thermofilu*m sp. Front Bioeng Biotechnol 2021;9(679):711487.
[9] Wu H, Chen M, Guang C, Zhang W, Mu W. Identification of a novel recombinant D-lyxose isomerase from *Thermoprotei archaeon* with high thermostable, weak-acid and nickel ion dependent properties. Int J Biol Macromol 2020;164:1267–74.
[10] Wu H, Chen M, Guang C, Zhang W, Mu W. Characterization of a recombinant D-mannose-producing D-lyxose isomerase from Caldanaerobius polysaccharolyticus. Enzym Microb Technol 2020;138:109553.
[11] Zhang W, Huang J, Jia M, Guang C, Zhang T, Mu W. Characterization of a novel D-lyxose isomerase from *Thermoflavimicrobium dichotomicum* and its application for D-mannose production. Process Biochem 2019;83:131–6.
[12] Guo Z, Long L, Ding S. Characterization of a D-lyxose isomerase from *Bacillus velezensis* and its application for the production of D-mannose and L-ribose. Amb Express 2019;9(1):149.
[13] Yu L, Zhang W, Zhang T, Jiang B, Mu W. Efficient biotransformation of D-fructose to D-mannose by a thermostable D-lyxose isomerase from *Thermosediminibacter oceani*. Process Biochem 2016;51(12):2026–33.
[14] Park CS, Yeom SJ, Lim YR, Kim YS, Oh DK. Substrate specificity of a recombinant D-lyxose isomerase from *Serratia proteamaculans* that produces D-lyxose and D-mannose. Lett Appl Microbiol 2010;51(3):343–50.
[15] Jumper J, Evans R, Pritzel A, Green T, Figurnov M, Ronneberger O, Tunyasuvunakool K, Bates R, Zidek A, Potapenko A, Bridgland A, Meyer C, Kohl SAA, Ballard AJ, Cowie A, Romera-Paredes B, Nikolov S, Jain R, Adler J, Back T, Petersen S, Reiman D, Clancy E, Zielinski M, Steinegger M, Pacholska M, Berghammer T, Bodenstein S, Silver D, Vinyals O, Senior AW, Kavukcuoglu K, Kohli P, Hassabis D. Highly accurate protein structure prediction with AlphaFold. Nature 2021;596(7873):583–9.
[16] Laskowski RA, MacArthur MW, Moss DS, Thornton JM. PROCHECK: a program to check the stereochemical quality of protein structures. J Appl Crystallogr 1993;26(2):283–91.
[17] Jones BJ, Kan CNE, Luo C, Kazlauskas RJ. Chapter Six - consensus Finder web tool to predict stabilizing substitutions in proteins. In: Tawfik DS, editor. Methods in enzymology. Academic Press; 2020. p. 129–48.
[18] Goldenzweig A, Goldsmith M, Hill SE, Gertman O, Laurino P, Ashani Y, Dym O, Unger T, Albeck S, Prilusky J, Lieberman RL, Aharoni A, Silman I, Sussman JL,

Tawfik DS, Fleishman SJ. Automated structure- and sequence-based design of proteins for high bacterial expression and stability. Mol Cell 2016;63(2):337–46.
[19] Musil M, Stourac J, Bendl J, Brezovsky J, Prokop Z, Zendulka J, Martinek T, Bednar D, Damborsky J. FireProt: web server for automated design of thermostable proteins. Nucleic Acids Res 2017;45(1):393–9.
[20] Chen J, Chen D, Chen Q, Xu W, Zhang W, Mu W. Computer-aided targeted mutagenesis of *Thermoclostridium caenicola* D-allulose 3-epimerase for improved thermostability. J Agric Food Chem 2022;70(6):1943–51.
[21] Maier JA, Martinez C, Kasavajhala K, Wickstrom L, Hauser KE, Simmerling C. ff14SB: improving the accuracy of protein side chain and backbone parameters from ff99SB. J Chem Theor Comput 2015;11(8):3696–713.
[22] Darden T, York D, Pedersen L. Particle mesh Ewald: an Nlog(N) method for Ewald sums in large systems. J Chem Phys 1993;98(12):10089–92.
[23] Martoňák R, Laio A, Parrinello M. Predicting crystal structures: the parrinello-rahman method revisited. Phys Rev Lett 2003;90(7):075503.
[24] Lee S-J, Lee D-W, Choe E-A, Hong Y-H, Kim S-B, Kim B-C, Pyun Y-R. Characterization of a thermoacidophilic l-arabinose isomerase from *Alicyclobacillus acidocaldarius*: role of lys-269 in pH optimum. Appl Environ Microbiol 2005;71 (12):7888–96.
[25] Qu G, Zhu T, Jiang Y, Wu B, Sun Z. Protein engineering: from directed evolution to computational design (In Chinese). Chin J Biotechnol 2019;35(10):1843–56.
[26] Dotsenko AS, Pramanik S, Gusakov AV, Rozhkova AM, Zorov IN, Sinitsyn AP, Davari MD, Schwaneberg U. Critical effect of proline on thermostability of endoglucanase II from *Penicillium verruculosum*. Biochem Eng J 2019;152:107395.
[27] Sun Z, Liu Q, Qu G, Feng Y, Reetz MT. Utility of B-factors in protein science: interpreting rigidity, flexibility, and internal motion and engineering thermostability. Chem Rev 2019;119(3):1626–65.
[28] Dotsenko AS, Rozhkova AM, Zorov IN, Sinitsyn AP. Protein surface engineering of endoglucanase Penicillium verruculosum for improvement in thermostability and stability in the presence of 1-butyl-3-methylimidazolium chloride ionic liquid. Bioresour Technol 2020;296:122370.
[29] Chen M, Song F, Qin Y, Han S, Rao Y, Liang S, Lin Y. Improving thermostability and catalytic activity of glycosyltransferase from Panax ginseng by semi-rational design for rebaudioside D synthesis. Front Bioeng Biotechnol 2022;10:884898.
[30] Rennison A, Winther JR, Varrone C. Rational protein engineering to increase the activity and stability of IsPETase using the PROSS algorithm. Polymers 2021;13 (22):3884.
[31] Rothschild LJ, Mancinelli RL. Life in extreme environments. Nature 2001;409 (6823):1092–101.
[32] Wu H, Chen Q, Zhang W, Mu W. Overview of strategies for developing high thermostability industrial enzymes: discovery, mechanism, modification and challenges. Crit Rev Food Sci Nutr 2021:1–18.
[33] Zhou H, Yu H, Zhao X, Yang L, Huang X. Molecular dynamics simulations investigate the pathway of substrate entry active site of rhomboid protease. J Biomol Struct Dyn 2019;37(13):3445–55.
[34] Liu S, Wang Y, Kong D, Wu J, Liu Z. Enhancing the thermostability of d-allulose 3-epimerase from *Clostridium cellulolyticum* H10 via directed evolution. Syst. Microbiol. Biomanuf. 2022;2(4):685–94.